Earth Planet. Sci. Lett. 678 (2026) 119809

Contents lists available at ScienceDirect

Earth and Planetary Science Letters

journal homepage: www.elsevier.com/locate/epsl

First-year sea ice history in the Arctic Ocean inferred from ancient DNA of *Polerella glacialis* over the past 50,000 years

Kyle Michael James Mayers [a,*], Nele Manon Vollmar [a,b], Tristan Cordier [a], Agnes Katharina Maria Weiner [a], Juliane Müller [c], Aud Larsen [a], Stijn De Schepper [a,b]

[a] NORCE Research and Bjerknes Centre for Climate Research, Nygårdsgaten 112, 5008, Bergen, Norway
[b] University of Bergen and Bjerknes Centre for Climate Research, Jashnebakken 5, 5007, Bergen, Norway
[c] Alfred Wegener Institute, Helmholtz Centre for Polar and Marine Research, Am Alten Hafen 26, 27568, Bremerhaven, Germany

ARTICLE INFO

Editor: Dr Tristan Horner

Keywords:
Arctic Ocean
Cryosphere
Holocene
Last deglaciation
Polarella glacialis
sedaDNA

1. Introduction

Sea ice plays an important role in Arctic climate and marine ecosystems. It supports a diverse community of organisms, with many sea ice biota being widespread over the Arctic (Hop et al., 2020). This unique ecosystem is under threat as Arctic sea ice extent is declining (Flores et al., 2023), and multi-year sea ice is being replaced by younger, first-year sea ice in large parts of the Arctic Ocean (e.g. Comiso et al., 2008; Kwok, 2018). It has been shown that multi-year sea ice supports a more diverse plankton community than first-year sea ice, and that a decline in sea ice-associated protist diversity is directly related to the reduction in multi-year sea ice (Hop et al., 2020). Since this trend of declining sea ice is projected to continue (Jahn et al., 2024), the future Arctic may be mainly covered by first-year sea ice which will bring substantial changes to the Arctic ecosystem and sea ice plankton diversity (Deb and Bailey, 2023; Kauko et al., 2018).

Determining how sea ice has changed through time is important for understanding the future of the Arctic. The satellite era only covers observations back to the late 1970s, providing too short a window for sea ice and Arctic ecosystem evolution. Longer records of Arctic climate change, and in particular sea ice change, have been derived from historical observations of whalers and polar expeditions (e.g. Walsh et al., 2017) as well as the marine sediment record which stores information about past sea ice conditions over long geological time scales. To reconstruct past sea ice conditions from the sediment record, we rely on a variety of proxies (e.g. de Vernal et al., 2013). Transfer functions defined from dinoflagellate cysts have been used to provide quantitative estimates of sea ice cover (e.g. Falardeau et al., 2018) while a combination of different biomarkers into a semi-quantitative index can differentiate between permanent or extended sea ice cover, marginal ice zones, variable sea ice cover, and open ocean (e.g. PIP_{25} index, Müller et al., 2011). In particular, the dinoflagellate *Polarella glacialis* is a well-known sea ice organism that is most abundant and frequent in first-year sea ice (Harðardóttir et al., 2024; Hop et al., 2020) and has been used in sedimentary ancient DNA (sedaDNA) records to reconstruct the history of first-year sea ice (Harðardóttir et al., 2024).

Polarella glacialis has two different life-stages, a motile vegetative cell stage and a spiny non-motile resting cyst stage (Montresor et al., 2003). Both the vegetative cells and cysts can be recovered from ice and have been observed in both Antarctic and Arctic sea ice (Harðardóttir et al., 2024; Hop et al., 2020; Kauko et al., 2018; Montresor et al., 1999; Stoecker et al., 1998). In studies of sea floor sediments, the cysts of *P. glacialis* have been overlooked and the species is in fact not included in modern palynological datasets from seafloor sediments (de Vernal et al.,

* Corresponding author.
E-mail address: kyma@norceresearch.no (K.M.J. Mayers).

https://doi.org/10.1016/j.epsl.2025.119809
Received 6 June 2025; Received in revised form 17 November 2025; Accepted 23 December 2025
Available online 9 January 2026

2020; Zonneveld et al., 2013). The cysts can easily be missed because of the preparation techniques used to extract palynomorphs from sediment. For example, palynological residues were in the past often sieved at too large a mesh size (*P. glacialis* cysts are usually <20 μm, Limoges et al., 2020), heated acids may have destroyed the fragile cysts (Harðardóttir et al., 2024), and/or the cysts could not be differentiated from other palynomorphs during routine analysis. There is also evidence that *P. glacialis* cysts are poorly preserved in marine sediments, despite representing a significant proportion of dinocysts in sediment traps during sea ice melt (Mäkelä et al., 2025). While a gentle palynological preparation (room temperature acids, sieving at 10μm) can make it easier to identify the cysts (e.g. De Schepper et al., 2019; Limoges et al., 2018), a more direct way to detect *P. glacialis* is using molecular assays targeted specifically to *P.* glacialis within sedaDNA records (De Schepper et al., 2019; Harðardóttir et al., 2024).

The highly sensitive droplet digital PCR (ddPCR) technique allows for reliable and precise detection of gene copies, even in low-concentration samples (Hindson et al., 2011). Additionally, ddPCR is robust against inhibitors often present in environmental DNA extracts, which can otherwise compromise PCR efficiency (Kokkoris et al., 2021). What is required to detect a specific organism is a unique molecular assay targeting a specific region of DNA. Such a region can be found with the ITS1 gene, which is present in multiple copies within the *P. glacialis* genome and has been used to determine the presence of *P. glacialis* in surface sediments and sediment cores around Greenland, and proposed as a proxy for first-year sea ice (De Schepper et al., 2019; Harðardóttir et al., 2024).

Here we analyse a sediment core from the Yermak Plateau, a region that today has an extensive sea ice cover and where Atlantic water flows into the Arctic Ocean. We reconstruct sea ice dynamics during the last ca. 50,000 years using biomarkers and a ddPCR assay of *P. glacialis* to discuss the evolution of the sea ice edge and occurrence of first-year sea ice.

2. Materials and methods

2.1. Materials

Our sediment core was collected in July 2021 during cruise KH21-234 with RV Kronprins Haakon to the Yermak Plateau and Arctic Ocean. The location of site KH21-234-34 (81.2199280 °N, 2.3710955 °E, 1011 m water depth; Fig. 1) on the western flank of the Yermak Plateau was chosen nearby site PS2837-5 (81.233333 °N, 2.381667 °E, 1023 m water depth (Jokat, 1999), where well-dated last glacial, deglaciation and Holocene sediments were recovered (Nørgaard-Pedersen et al., 2003; Vogelsang et al., 2003) and several paleoceanographic studies were conducted (e.g., Müller et al., 2009). The new sediment core was collected to retrieve fresh, unsampled and uncontaminated sediment from this location for different ancient DNA studies (including metabarcoding and ddPCR).

We retrieved 454 cm of sediment in gravity core KH21-234-34GC. Following retrieval, the core was manually cut into four sections of 69,130, 130, and 125cm, the core liners cleaned with bleach, capped, and stored on board at 4°C. Cores were transported and stored cooled until they were opened and split in the ancient DNA lab at NORCE in Bergen (Norway). The sediment recovered from KH21-234-34GC was a homogenous brownish grey, silty clay (0–225 cm), brownish grey to dark grey, very fine sandy clay (225–329 cm), alternating brown, light grey and dark grey, very fine sandy clay (329–387 cm) and grey clay (387–454 cm). The lithological description of PS2837-5 (Stein et al. 2003) describes dark olive grey clayey silt/silty clay for most of the upper 500 cm, and a sandier clayey silt/silty clay between 386 and 453 cm.

2.2. Methods

2.2.1. Physical properties

Prior to opening the KH21-234-34GC sections, we measured the magnetic susceptibility at 1 cm resolution using a Bartington MS2C loop sensor (Ø 125mm) with a Geotek Multi-Sensor Core Logger (MSCL-S).

2.2.2. Radiocarbon ages

After KH21-234-34GC was split in the ancient DNA lab (details below), one half was sampled for radiocarbon dating and we picked shells of the planktic foraminifer *Neogloboquadrina pachyderma* at four depths (see Table 2). We obtained accelerator mass spectrometry (AMS) ^{14}C dates from the radiocarbon lab at ETH Zurich. The functions BchronCalibrate:sampleAges and Bchronology:PredictAges were used

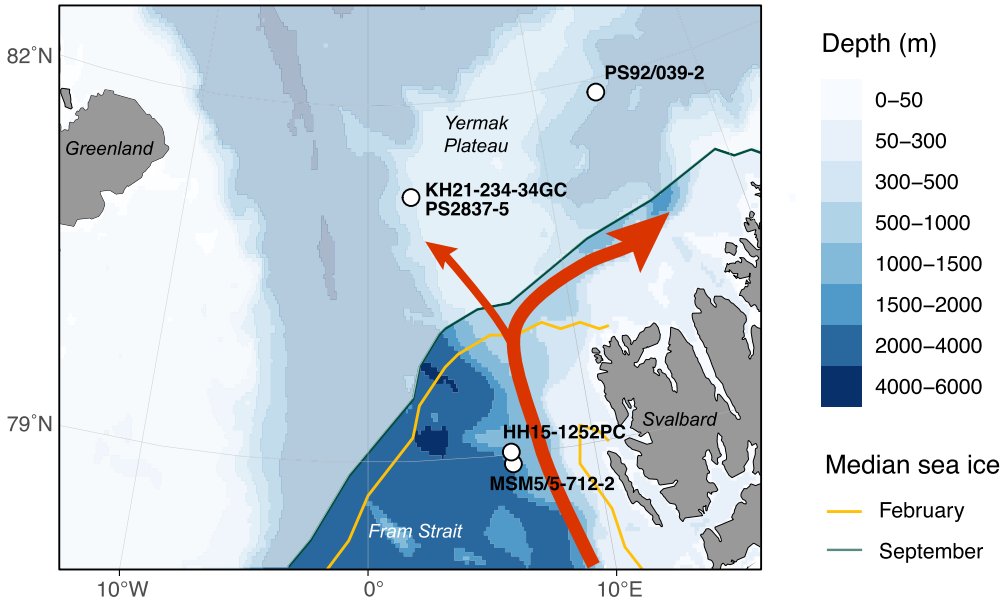

Fig. 1. Location of our study area. Location of our study site KH21-234-34, a re-occupation of site PS2837-5, and other sites discussed in the text. Red arrow indicates the warm water West Spitsbergen Current. Green line and white shading indicate the summer sea ice extent, yellow line is the winter sea ice extent (Stroeve and Meier, 2018).

from the statistical package BChron (version 4.7.7; Haslett and Parnell, 2008) to calculate calibrated ages. For calibration, we applied the Marine20 calibration curve (Heaton et al., 2020) and no other correction. Ages reported in Nørgaard-Pedersen et al. (2003) from sediment core PS2837-5 were also recalculated using the same method and calibration curve.

2.2.3. Paleogenomics: DNA extraction and digital droplet PCR

DNA was extracted from the gravity core sections at the ancient DNA laboratory at NORCE, located in Bergen, Norway. Strict protocols were followed to eliminate contamination from modern DNA. Gravity core sections were opened, and one half was sampled with sterile syringes at 10 cm depth intervals throughout most of the core, and up to 3 cm intervals during periods of expected climate transitions identified using magnetic susceptibility data. A sampling control was taken during this time, consisting of a tube containing Milli-Q water left open in the lab. DNA was extracted from 8.1 to 8.8g of sediment using the DNeasy PowerMax Soil Kit (Qiagen) following manufacturer's instructions, with DNA being eluted into 5 mL elution buffer and stored at -20°C until analysis. While weighing out the sediment for DNA extraction we obtained a subsampling control which again consisted of an open tube with 1 mL Milli-Q water. A total of 6 sampling, subsampling, and extraction controls underwent DNA extraction to control for contamination from modern DNA.

Droplet digital PCR (ddPCR) was conducted using a QX200 Droplet Digital PCR system (Bio-Rad) targeting the ITS1 region of the sea-ice-associated dinoflagellate *Polarella glacialis*. ddPCR reactions were run at a final volume of 20 μL, using 5 μL of template DNA, 1x EvaGreen supermix (Bio-Rad), 250 nM of forward primer Polarella-ITS-44F (5'-CGACTGGGTGGAGATGGTTG-3') and reverse primer Polarella-ITS-138R (5'-CCCAGGTGTTTAAGCCAGGT-3') (De Schepper et al., 2019). PCR reactions were emulsified with QX200 Droplet Generation Oil for EvaGreen using the QX200 Droplet Generator (Bio-Rad Laboratories). Droplets were transferred into a ddPCR 96-well plate and sealed with pierceable sealing foil using a PX1 PCR plate sealer (Bio-Rad Laboratories). PCR reactions were conducted in a C1000 touch thermocycler with deep-well module (Bio-Rad) using the following program: 95°C for 5 min; 40 cycles of 95°C for 30 s then 62°C for 1 min; 4°C for 5 min; 90°C for 10 min; 4°C infinite hold. Plates were equilibrated to room temperature for 10-15 minutes prior to analysis on the QX200 droplet reader (Bio-Rad). In each ddPCR run, negative non-template controls (NTC) of ultrapure water and positive controls containing DNA from cultured *P. glacialis* CCMP1383 were included and used to set thresholds between positive and negative droplets, and to check for possible PCR inhibitors present in DNA extracts. Thresholds were set to include droplets with high fluorescence in positive controls but not those with lower fluorescence in the NTCs. No *P. glacialis* was observed in any of the NTCs, sub-sampling, sampling or extraction controls, and no inhibition of droplet amplitude was detected in sedaDNA samples.

2.2.4. PIP_{25} index

Previously published IP_{25} and brassicasterol concentrations measured in the neighbouring core PS2837-5 (Müller et al., 2009; Birgel and Hass, 2004) were used to calculate the P_BIP_{25} index according to Müller et al. (2011):

(1) $P_BIP_{25} = IP_{25}/(IP_{25} + \text{brassicasterol x c})$, with;
(2) c = mean IP_{25} concentration/mean brassicasterol concentration.

As outlined by Müller and Stein (2014), PIP_{25} values determined for samples with simultaneously low biomarker concentrations close to or below the detection limit (in PS2837-5: $IP_{25} < 0.05$ μg/g; brassicasterol < 0.05 μg/g) – indicative of a permanent sea ice cover – may lead to an underestimation of the sea ice coverage and for those samples the index was accordingly set to 1.

3. Results

3.1. Correlation and age model

3.1.1. Correlating PS2837-5 and KH21-234-34GC using physical properties

We used magnetic susceptibility data to correlate both gravity cores, with the aim to transfer the age model from PS2837-5 to our studied core. To align the PS2837-5 data (Niessen, 2000) with our new KH21-234-34 data, we used QAnalyseries (v.1.5.4) and set KH21-234-34 as the target. We used 12 tie points to align both records, which gave a correlation of r=0.962 (Table 1, Fig. 2). This correlation is further corroborated by the lithology of both cores. In 34GC (329–387 cm) and in PS2837-5 (386–453 cm), an interval of brown to grey, sandy clay/silt has been described. Transferring the depths of this interval (386–453 cm) from PS2837-5 to the KH21-234-34GC depth scale returned values of 325–383 cm, almost identical to the depth of this interval in KH21-234-34GC (329–387 cm).

3.1.2. Age model

Following the correlation of the magnetic susceptibility of both records, we transferred the sample depths of the radiocarbon dates from PS2837-5 (Nørgaard-Pedersen et al., 2003) to the KH21-234-34GC depth scale (Table 2). We observed an age reversal between PS2837-5 sample KIA7571 (199.98 cm) and KH21-234-34GC sample 118424.1.1 (199.00 cm), samples that were 2 cm apart on the combined KH21-234-34GC depth scale. Both ages were included in the Bayesian age model. The sample at 454 cm, with a radiocarbon age outside the marine20 calibration range, was also included in making the Bayesian age model (Table 2, Fig. 3).

Our 454-cm long sediment core from the Yermak Plateau recovered sediment dating back ca. 50,000 years (Fig. 3). Our proxy data therefore cover part of MIS 3, the Last Glacial Maximum (19,000–23,000 cal yr BP), the Last Glacial termination including the Bølling-Allerød and the Younger Dryas, and the Holocene. Samples for molecular analysis were collected at different depths to have a generally uniform time resolution with increased resolution across the different climate intervals (i.e. Bølling-Allerød, Younger Dryas).

We acknowledge that the biomarker and Pgla-DNA were not measured on the same cores. However,the correlation based on the magnetic susceptibility and lithology between both cores is very solid (r=0.962), indicating that differences in timing between Pgla-DNA and biomarker trends are robust on centennial timescales, based on our age model.

3.1.3. Polarella glacialis-DNA in KH21-234-34GC

We quantified the number of gene copies of *P. glacialis* (=Pgla-DNA; Fig. 4a) across three replicate reactions of each DNA sampled for each sediment depth. To be considered a positive detection, at least 2 out of the 3 replicates must be positive. Nineteen samples had zero positive

Table 1
Depth correlation tie-points between KH21-234-34GC and PS2837-5 based on magnetic susceptibility.

PS2837-5 Depth (cm)	*KH21-234-34 Depth (cm)*
21	10
102	75.2
181	133.2
263	207.6
292	235.6
330	274.6
365	305.6
399	338
418	352
467	396
487	410
513	425

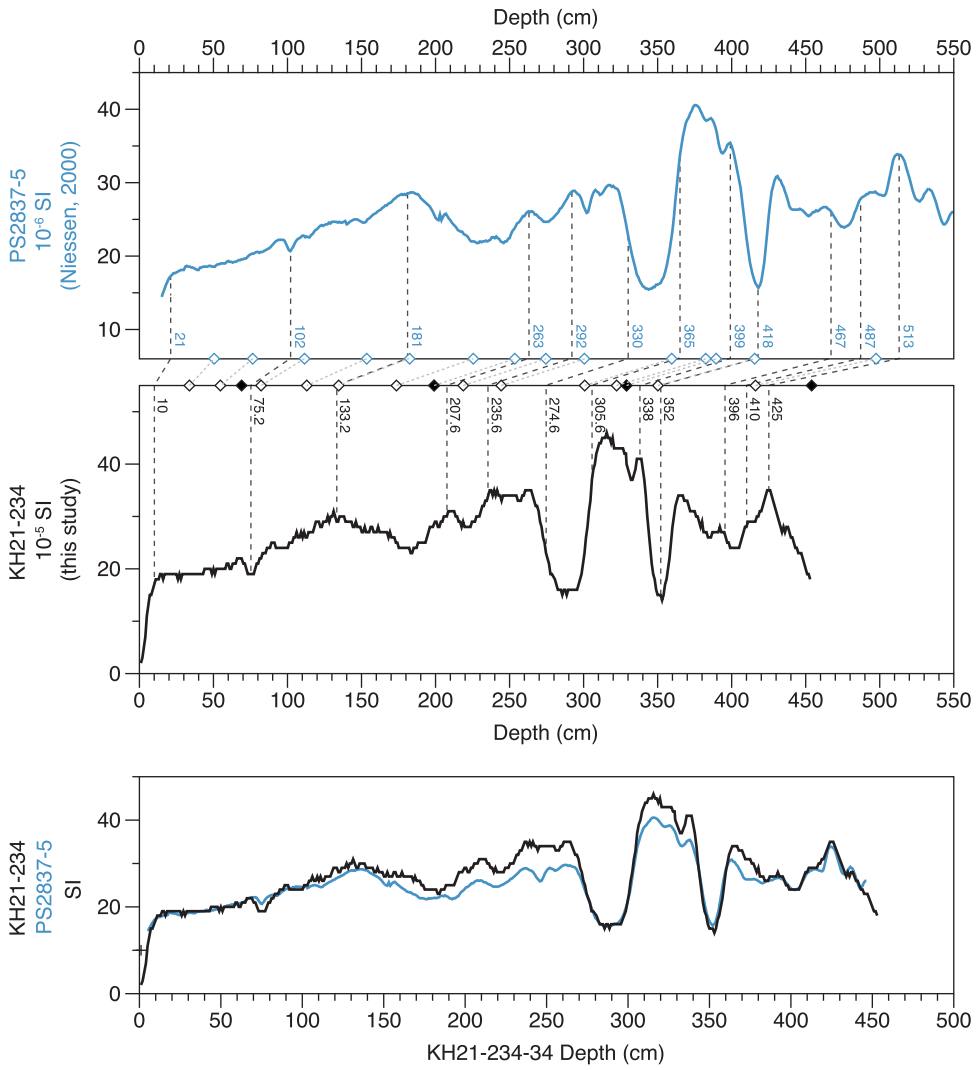

Fig. 2. Magnetic susceptibility records from cores PS2837-5 and KH21-234-34GC. Magnetic susceptibility records from PS2837-5 (Niessen 2000) and KH21-234-34GC (this study), including the correlation tie points that tie PS2837-5 to KH21-234-34GC. Filled diamonds indicate where samples for 14C were collected, and empty diamonds tie points. *Lowermost panel* shows both magnetic susceptibility records on the depth scale of KH21-234-34GC.

detection in all three replicates (Fig. 4b, yellow dots), and 6 samples (430, 380, 370, 327, 302 and 262 cm) had only 1 positive detection and were therefore set to 0 for further analyses (Fig. 4b, orange dots). The oldest detection of Pgla-DNA was at 440 cm downcore (46.8 cal kyr BP) with an average of 15.1 copies g^{-1} sediment (Suppl. Fig. 1). Between the bottom of the core at 450 cm (48.1 cal kyr BP) and 262 cm core depth (13.7 cal kyr BP), only 7 of the 30 samples contained Pgla-DNA or were at the detection limit (determined as ~10 gene copies g^{-1} sediment). Within this depth range, a notable increase in gene copies was observed at 308 cm (15.4 cal kyr BP) with an average of 101.6 copies g^{-1} sediment.

From 258 cm (13.7 cal kyr BP) until the top of our sediment core at 10 cm (0.3 cal kyr BP) 36 of the 38 samples contained detectable Pgla-DNA, with only 225 cm and 215 cm having undetectable values (13.2 and 12.7 cal kyr BP respectively). At 255 cm (13.7 cal kyr BP), a relatively high Pgla-DNA concentration was observed (average 107.9 copies g^{-1} sediment). From 250 cm to 177cm (13.6 to 9.7 cal kyr BP), gene copies were variable but within similar ranges (averages 12.2–71.9 copies g^{-1} sediment). From 170 cm (9.2 cal kyr BP) to the top of the sediment core there was a general increasing trend in Pgla-DNA, with a peak of 171.9 copies g^{-1} sediment at 10 cm (0.3 cal kyr BP). The topmost sediment sample had an average copy number of 105.1 copies g^{-1} sediment.

3.1.4. *Biomarker record from PS2837-5*

The P_BIP_{25} index (Fig. 5), based on combining the highly branched isoprenoid biomarker IP_{25} ("Ice Proxy with 25 carbon atoms") and open water biomarker brassicasterol, generally indicates a multi-year ice cover ($P_BIP_{25} = 1$) between 370 and 320 cm core depth (32.0 – 17.6 cal kyr BP). This is briefly interrupted by an increase in IP_{25} and a resulting P_BIP_{25} index of 0.5–0.6 around 350 cm (28.3 cal kyr BP), suggesting seasonal sea ice or marginal ice zone conditions. Both IP_{25} and brassicasterol are detected in almost all subsequent samples between 32 and 320 cm (1.6 and 17.6 cal kyr BP respectively), and the P_BIP_{25} index fluctuated between 0.3 and 0.8, indicating a seasonal sea ice cover or marginal ice zone region on the Yermak Plateau. There are two exceptions to this pattern. Between 288 and 300 cm (13.9 – 14.3 cal kyr BP) brassicasterol was abundant while IP_{25} was absent suggesting open waters, corresponding to the Bølling-Allerød. Between 209 and 212 cm (12.4 – 12.7 cal kyr BP) both IP_{25} and brassicasterol were absent suggesting a brief return to permanent sea ice cover in the Younger Dryas. In the upper 200 cm of the records, the P_BIP_{25} ratio increases gradually, suggesting an increase in sea ice extent from the early to the late Holocene.

Table 2
Radiocarbon and calibrated ages for PS2837-5 and KH21-234-34GC, and Bayesian age model for KH21-234-34GC using marine20 calibration curve and no reservoir correction. Calibrated ages are shown with 2.5% and 97.5% probabilities.

								Calibrated ages			Age Model	
PS2837-5 Depth (cm)	KH21-234-34GC Depth (cm)	Depth (cm) on KH21-234-GC scale	14C AMS (yr)	error (±yr)	Sample ID	Reference	Calibration curve	Age (cal yr BP) 2.5%	Age (cal yr BP)	Age (cal yr BP) 97.5%	Depth (cm) on KH21-234-GC scale	Age (cal yr BP) median
0		0	0	1	Top		normal	-2	0	2	0	0
50.5		33.75	1730	40	KIA4652	Nørgaard-Pedersen et al., (2003)	marine20	970	1128	1264	33.75	1139
76.5		54.67	2940	35	KIA8927	Nørgaard-Pedersen et al., (2003)	marine20	2365	2547	2697	54.67	2543
	69.0	69.00	4410	62	118423.1.1	*this study*	marine20	4145	4371	4601	69.00	4293
111.5		82.17	4565	45	KIA8928	Nørgaard-Pedersen et al. (2003)	marine20	4396	4580	4780	82.17	4733
153.5		113.01	7005	45	KIA8929	Nørgaard-Pedersen et al. (2003)	marine20	7164	7319	7464	113.01	7308
182.5		134.56	7670	60	KIA4653	Nørgaard-Pedersen et al. (2003)	marine20	7758	7945	8134	134.56	7956
225.5		173.58	8890	60	KIA8930	Nørgaard-Pedersen et al. (2003)	marine20	9189	9395	9534	173.58	9403
253.5		198.98	10540	50	KIA7571	Nørgaard-Pedersen et al. (2003)	marine20	11371	11629	11871	198.98	11450
	199.0	199.00	10252	98	118424.1.1	*this study*	marine20	10888	11219	11568	199.00	11503
274.5		218.70	11755	60	KIA10863	Nørgaard-Pedersen et al. (2003)	marine20	12884	13075	13258	218.70	13051
300.5		244.32	12255	60	KIA7572	Nørgaard-Pedersen et al. (2003)	marine20	13406	13600	13797	244.32	13576
359.5		300.73	12540	70	KIA10864	Nørgaard-Pedersen et al. (2003)	marine20	13728	13951	14231	300.73	14016
382.5		322.28	15640	80	KIA10865	Nørgaard-Pedersen et al. (2003)	marine20	17825	18099	18400	322.28	18101
389.5		328.95	17040	110	KIA4654	Nørgaard-Pedersen et al. (2003)	marine20	19328	19669	20031	328.95	19877
	329.0	329.00	17479	149	118425.1.1	*this study*	marine20	19767	20202	20603	329.00	19937
415.5		350.16	23830	180	KIA7573	Nørgaard-Pedersen et al. (2003)	marine20	26819	27207	27584	350.16	27208
497.5		416.06	48760	4810	KA4655	Nørgaard-Pedersen et al. (2003)	marine20	43215	49943	54719	416.06	43093
	454.0	454.00	55500	10947	118426.1.1	*this study*	marine20	37850	48890	54717	454.00	49061

4. Discussion

4.1. Interpreting Pgla-DNA as a first-year sea ice indicator

P. glacialis is a well-documented sea ice organism that has a bipolar distribution (Marret et al., 2020) and observations in Arctic and Antarctic sea ice suggest that it thrives best in first-year sea ice. A large survey of sea ice organisms in >100 first-year and multi-year Arctic sea ice cores found that *P. glacialis* is both more abundant and more frequently present in first-year sea ice compared to multi-year ice (Hop et al., 2020). Like most dinoflagellates recorded in sea ice, *P. glacialis* is most abundant in the upper part of sea ice (Gradinger et al., 1999; Kauko et al., 2018; Stoecker et al., 1998; Werner et al., 2007).

Both the motile vegetative cells and resting cysts were abundantly present early in the season (Kauko et al. 2018), prior to major sea-ice melt. These observations are further supported by sea ice studies from Baffin Bay and around Greenland, where *P. glacialis* is recorded in first-year sea ice, but not in multi-year ice (Harðardóttir et al., 2024), and a clear link demonstrated between sea ice melt and *P. glacialis* cysts within sediment traps from around the Arctic, including Svalbard and Greenland (Harðardóttir et al., 2024; Mäkelä et al 2025). In addition, a positive relationship between sea ice concentration was observed for sites with up to 80% annual sea-ice cover, and a negative relationship with an annual sea-ice cover >80 – 100% (Harðardóttir et al., 2024), indicating greater *P. glacialis* abundance in seasonal sea ice. These authors suggest that Pgla-DNA is a first-year sea ice indicator, and also metabarcoding studies have linked the relative abundance of *P. glacialis* DNA to spring sea-ice conditions in Antarctic coastal regions and fjords (Boere et al., 2009; Pieńkowski et al., 2024). We agree with previous work and have interpreted the presence of Pgla-DNA in our study to reflect first-year sea ice.

4.2. Pgla-DNA preservation and gene copy variation

DNA is subject to degradation over time just like other biomolecules (Dell'Anno & Corinaldesi, 2004), but our *Pgla*-DNA record is more likely attributable to an environmental rather than a preservation signal. In theory, if DNA degradation were a significant factor, we would expect a stronger signal in the top layers of the sediment core and greater degradation with a weaker signal at deeper levels. Our record shows indeed a decreasing trend in gene copy concentrations with age over the past ~8,000 years, however, comparable gene copy concentrations are detected at the top of the sediment core (e.g. at 10 cm, 0.3 cal kyr BP) and at deeper depths (255 and 308 cm, 13.7 and 15.4 cal kyr BP respectively). If the Pgla-DNA degrades with time, these major peaks in the Pgla-DNA gene copy concentrations that reach values as high as more modern sediments cannot be the result of poor preservation. Rather, this observation strongly suggests that DNA degradation does not play a major role over the timescales examined here and that the trends and variability of Pgla-DNA are environmental signals. In addition, our Pgla-DNA signal matches well with IP_{25} concentrations, suggesting preservation issues are very likely not interfering with our ecological signal.

One complication is that the variation in gene copy numbers in a dinoflagellate cell may be very large, because they possess multiple copies of certain marker genes (e.g., 18s ribosomal genes) within their

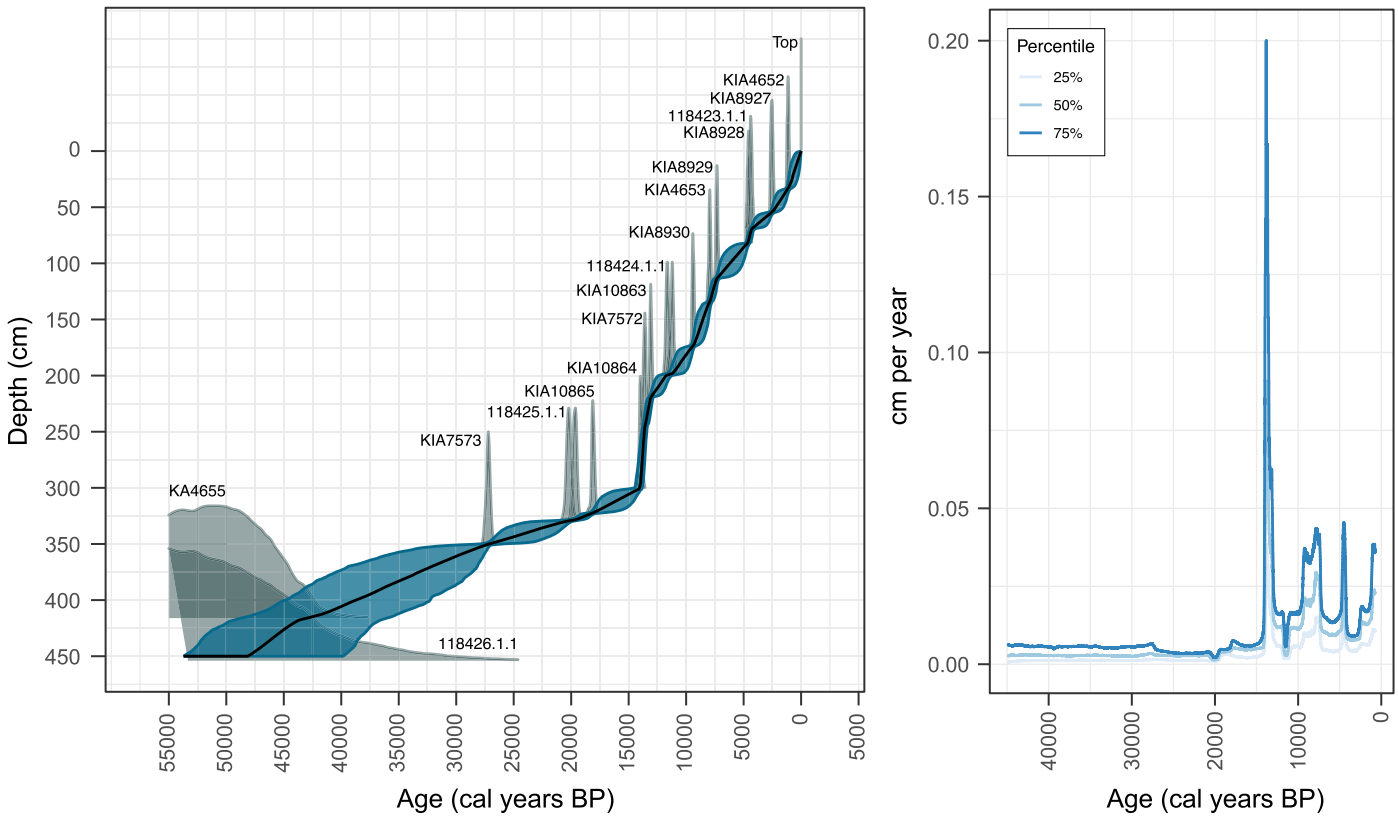

Fig. 3. Age model and accumulation rates for core KH21-234-34GC. (left). Age model (left) and accumulation rates (right) for KH21-234-34.

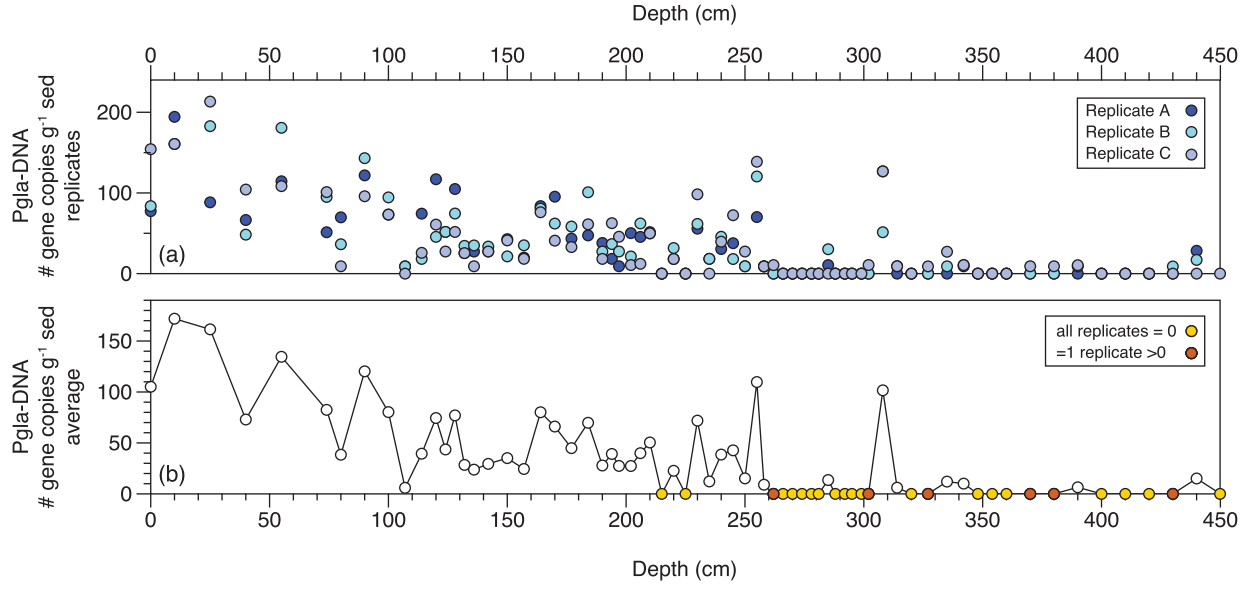

Fig. 4. Genetic data for Polarella glacialis from core KH21-234-34GC. (a) Gene copies per gram sediment of *Polarella glacialis* (Pgla-DNA) in each of the three replicates per sample. If only one or two points are visible it is because of the same copy number in replicates being determined. **(b)** Average of the replicates, with orange dots representing samples where all three replicates returned zeros. Orange dots show data points that had only 1 positive replicate, but which we considered as zero.

genomes (Godhe et al., 2008; Zhu et al., 2005). A larger amount of DNA per cell enhances the detectability, but on the other hand it also complicates the interpretation of the variation in gene copy numbers, which may be a function of the number of cells reaching the sea floor, or the amount of gene copies in any given cell. Intraspecific variation – variability of characteristics among individuals of the same species - in gene copy numbers in response to environmental change can also complicate this relationship (Lavrinienko et al., 2021; Krabberød et al., 2025), and differences due to the ploidy (number of sets of chromosomes in an organism) between vegetative and encysted dinoflagellate cells (Figueroa et al., 2015). This relationship requires further investigation, but we acknowledge it may bias our interpretations.

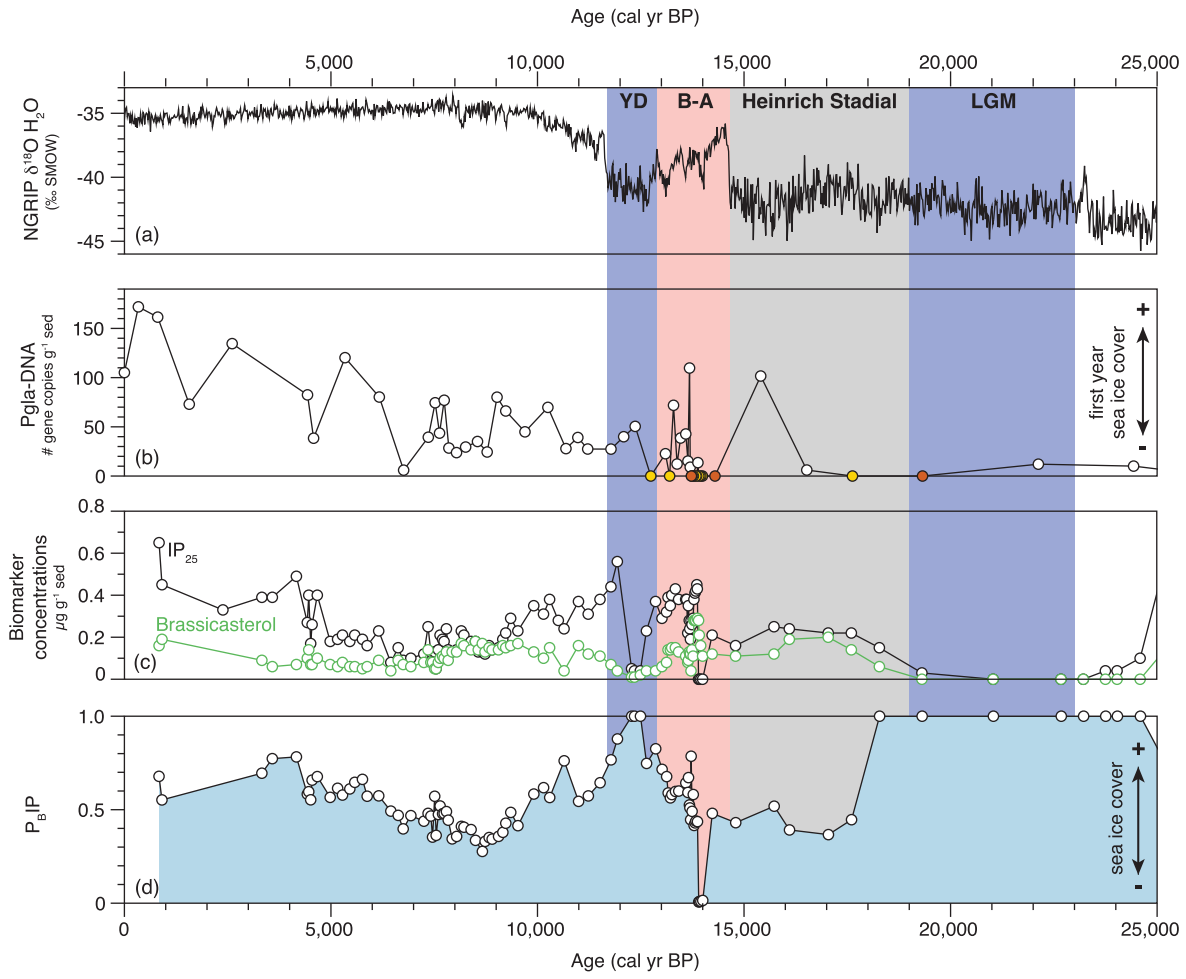

Fig. 5. Paleo context of genetic data of *P. glacialis* and biomarkers. (a) NGRIP ice core water isotope ratios (Veres et al., 2013) as a reference for the climate conditions across the studied time interval, **(b)** Pgla-DNA gene copy concentrations in KH21-234-34GC. Average of the three replicates (white), with yellow dots representing samples where all three replicates were zero, orange dots show data points that had only 1 positive replicate, but which we considered as zero. **(c)** IP_{25} (black; Müller et al., 2009) and brassicasterol (green; Birgel and Hass, 2004) accumulation rates for PS2837-5 on the KH21-234-34GC depth scale. **(d)** P_BIP_{25} ratio for PS2837-5.

4.3. Stratigraphic range and abundance of Pgla-DNA in Arctic sediments

The Pgla-DNA and published fossil (cyst) stratigraphic record are both showing that *P. glacialis* is present since Marine Isotope Stage (MIS) 3 in the Arctic. The oldest record of Pgla-DNA in the core KH21-234-34GC dates to 46.8 cal kyr BP which corresponds to a depth of 440 cm in the core (Suppl. Fig. 1). However, this age should be treated carefully, as the ^{14}C AMS calibrated age of the sample at 454 cm falls outside the Marine20 calibration curve, thus possibly suggesting an age >55 cal kyr BP. Nevertheless, the oldest occurrence of Pgla-DNA at our site is in MIS 3, which is in agreement with a ddPCR study from the East Greenland Sea (De Schepper et al., 2019) and its record as fossilized cysts (Limoges et al., 2020). In addition, *P. glacialis* is documented in surface sediments from Baffin Bay and East Greenland (Harðardóttir et al., 2024; Mäkelä et al., 2025), Hudson Bay (Heikkilä et al., 2014) and from the Yermak Plateau (K. Mayers, unpubl. data). The cysts are nevertheless reported from modern and Holocene sediments (De Schepper et al., 2019; Harðardóttir et al., 2024; Limoges et al., 2018).

The recovered range of Pgla-DNA per gram of sediment in KH21-234-34GC (0–213 copies g^{-1} sediment) was comparable to downcore samples from an East Greenland Sea sediment core. There, in a record spanning the last ca.100,000 years, <40–266 copies g^{-1} sediment was recorded, with one exceptional sample at ~34 kya which had considerably higher copy numbers (>1000 copies g^{-1} sediment; De Schepper et al., 2019). A sediment core from the Baffin Bay dating back ~10,000 years recorded higher *P. glacialis* copy numbers between 106–33,057 copies g^{-1} sediment (Harðardóttir et al., 2024). The differences can be related to the different sea ice conditions in those areas. Our core was collected at a water depth (1011m) like the East Greenland (1610 m) and Baffin Bay (963 m) cores, but these latter locations are today characterized by strong seasonal sea ice fluctuations (Walsh et al., 2017; Fetterer et al., 2017). In contrast, our study site is located north of the median summer sea ice edge today and in the past (Müller et al., 2009; Xiao et al., 2015). Such an environment likely corresponds to more multi-year ice, a habitat that is less favoured by *P. glacialis* (see 4.1 discussion). Moreover, the Yermak Plateau experiences less sea ice melting compared to Baffin Bay and East Greenland where the summers are ice-free, and less opportunity for cysts to sink to the seafloor following the seasonal sea ice melt. Keeping this in mind, less gene copies of Pgla-DNA can be expected in Yermak Plateau sediments compared to Baffin Bay and East Greenland.

4.4. Arctic Ocean paleoceanography

During MIS 3 and the LGM, we conclude that the Yermak Plateau was generally characterized by a multi-year sea ice cover, limited first-year sea ice and minimal ice melting. This we interpret from the general absence of detecting Pgla-DNA gene copies, although occasional low

concentrations are recorded (Fig. 5b, Suppl. Fig. 1). Zero or very few Pgla-DNA gene copies in the sediment can also be interpreted as an open ocean setting with too warm conditions for sea ice to form and *P. glacialis* to live, but this is a highly unlikely environment for the glacial Arctic Ocean. Indeed, several studies from the Yermak Plateau have shown a multi-year permanent sea ice cover during this time interval (Kremer et al., 2018; Müller et al., 2009; Müller and Stein, 2014; Xiao et al., 2015), congruent with the low biomarker concentrations and a P_BIP_{25} ratio of one this study.

On the eastern Yermak Plateau, a marginal sea ice setting with a coastal polynya was likely established after ca. 30 kyr ago (Fig. 1; PS92/039-2; Kremer et al., 2018), whereas further south in the Fram Strait, spring sea ice was still extensively present (El bani Altuna et al., 2024). On the western Yermak Plateau, between 32 and 18 kyr, a permanent sea ice cover mostly occurred as expressed in the absence of IP_{25} (Müller et al., 2009), a P_BIP_{25} index of one and the absence of Pgla-DNA (this study). The near absence of Pgla-DNA on the western Yermak Plateau is thus most compatible with an environment with a dominant multi-year sea ice cover and limited first-year sea ice. Furthermore, the area likely experienced mainly freezing conditions and little sea ice melt. Indeed, for Pgla-DNA to arrive in the sediment, the sea ice it inhabits needs to melt. Between 27–25 cal kyr BP, the sea ice margin may have been close to our study site (Müller et al., 2009), but we detected no Pgla-DNA in the only sample analysed in this interval.

A major change in the Yermak Plateau Sea ice cover is observed between 18.2 and 17.6 cal kyr BP when the permanent sea ice cover broke up and multi-year sea ice was likely flushed out of the Arctic Ocean. This change is evidenced by the rapid decrease in the P_BIP_{25} index (Fig. 5d). The low biomarker concentrations (Fig. 5c) suggest a considerable multi-year sea ice cover in a marginal ice zone, and the absence of Pgla-DNA until 17.6 cal kyr BP (Fig. 5b) indicates that no first-year sea ice occurred. This implies that there was little transfer of surface ocean signals, biomarkers and DNA, to the sea floor, or in other words, that limited melting of sea ice occurred. Sea ice melting would most likely occur very late in the summer season, when sea ice extent is retreated to its minimum. We thus interpret the Yermak Plateau environment to be without first-year sea ice during this time interval, and rather dominated by multi-year sea ice that likely was being flushed out of the Arctic Ocean via the Fram Strait.

Substantial evidence of first-year sea ice first appears around 15.4 cal kyr BP on the Yermak Plateau, when Pgla-DNA shows a major peak (Fig. 5b). Increasing IP_{25} and brassicasterol in core PS2837-5 (Fig. 5c; Müller et al. 2009) and further south in the Fram Strait (El bani Altuna et al., 2024) also point to a shift from an extensive sea ice cover towards a marginal sea ice cover ca.16 cal kyr BP. This is likely related to increased inflow of warm Atlantic Water (El bani Altuna et al., 2024), which extended onto the Yermak Plateau (Hald & Aspeli, 1997). Stronger inflow of warmer water, likely led to more sea ice melt on the Yermak Plateau and the formation of first-year sea ice in a multi-year sea ice environment, a setting not unlike today.

The Bølling-Allerød (14.7–12.9 cal kyr BP), an abrupt climate warming event that is well recorded in ice cores on Greenland (Fig. 5a), showed rapid changes from seasonal sea ice cover (14.7 to 13.9 cal kyr BP) to open waters (13.9–14.0 cal kyr BP) and again seasonal sea ice (13.9 to 12.9 cal kyr BP) on the Yermak Plateau. Such strong variations in sea ice cover are also seen further south in the Fram Strait around this time (El bani Altuna et al., 2024; Falardeau et al., 2018; Müller and Stein 2014). There, the sea ice cover fluctuates from nearly sea ice free to an extensive sea ice cover and back to a reduced sea ice cover at site MSM5/5-712 (Falardeau et al., 2018), whereas the nearby site HH15-1252 shows a very reduced, marginal spring sea ice cover early on followed by a return to a more established spring sea ice cover (El bani Altuna et al., 2024). This is also the time when meltwater pulse 1A occurred (ca. 14.6 cal kyr BP, Brendryen et al., 2020; Lucchi et al., 2015), an interval that is not obviously present at our study site. Nevertheless, large variability is shown in the different sea ice proxies at the Yermak Plateau. In the earliest part of the Bølling-Allerød, 14.7 to 13.9 cal kyr BP, a seasonal sea ice cover occurred on the eastern Yermak Plateau. Around 14.0–13.9 cal kyr BP, a short-lived year-round, ice-free, open ocean occurred (Fig. 5d). Pgla-DNA was not detected, indicating no first-year sea ice formation and/or melting in the area (Fig. 5b) during this entire period. In the later part of the Bølling-Allerød, after 13.9 cal kyr BP, a seasonal sea ice cover is installed again (Fig. 5d) and from this time onwards, we recorded variable concentrations of Pgla-DNA in several samples (Fig. 5b) indicating the presence of first-year sea ice. Here, the higher concentrations of open ocean and sea ice biomarkers (Fig. 5c) and the presence of Pgla-DNA in the sediment indicate that sea ice melted in this region, including first-year sea ice.

In the Younger Dryas (12.9–11.7 cal kyr BP), an abrupt cooling event following the Bølling-Allerød (Fig. 5a), three out of four studied samples recorded Pgla-DNA, indicating the presence of first-year sea ice. One sample (12.7 cal kyr BP) did not yield Pgla-DNA and can be interpreted as a permanent multi-year sea ice cover. The P_BIP_{25} index across the Younger Dryas indicates a multi-year sea ice cover, but later than Pgla-DNA, between 12.5 and 12.2 cal kyr BP. Thus, both proxies indicate multi-year sea ice during the cold Younger Dryas, but not at the same time. One explanation for this difference in timing could be because the two proxies were measured on different cores. Although the correlation of the magnetic susceptibility between PS2837-5 and KH21-234-34 is strong (r=0.962, Fig. 2), there could always be intervals where the correlation could be improved. Although the biomarkers and Pgla-DNA do not align in the detail, we still infer that a more severe sea ice cover was reinstated during the Younger Dryas (see also Müller et al., 2009; Müller and Stein, 2014). Such interpretation is consistent with the inference of a permanent sea ice cover to the north based on a foraminifer assemblage study from the southern Yermak Plateau, and reconstructions of a short-lived multi-year sea ice in the early part of the Younger Dryas further south in the Yermak Plateau (MSM5/5-712) (Chauhan et al., 2014; Falardeau et al., 2018; Müller and Stein, 2014).

The Holocene Yermak Plateau is characterised by a seasonal sea ice cover, which may consist mainly of first-year sea ice. We deduce this from the comparable trends in the P_BIP_{25} index and our Pgla-DNA proxy during the Holocene (Fig. 5b, d), which could imply that the seasonal sea ice on the Yermak Plateau consists for a large part of first-year sea ice, as opposed to seasonally drifted multi-year ice. In this view, the Pgla-DNA proxy provides an additional assessment of the reconstructed sea ice cover in this area.

The early Holocene P_BIP_{25} index suggests less and variable sea ice, while this gradually moves into a marginal sea ice cover during the late Holocene (P_BIP_{25} index > 0.5; cf. Müller et al. 2011). Pgla-DNA is continuously recorded in the Holocene, but remains variable during the early Holocene (ca. 6–9 cal kyr BP), and from around 5–6 cal kyr BP, Pgla-DNA increases steadily together with the P_BIP_{25} index. It thus appears that as the environment became cooler again during the late Holocene, the Yermak Plateau experienced a marginal sea ice setting with more first-year sea ice. In this interpretation the increasing trend in Pgla-DNA would reflect more first-year sea ice. This interpretation fits the P_BIP_{25} index and the regional cooling during the Late Holocene (Farnsworth et al., 2020; Rasmussen et al., 2012), as well as an early to late Holocene documented trend to a more extensive sea ice cover in the entire region, where also in the southern Fram Strait a lesser (seasonal) sea ice cover is reported in the early Holocene (Falardeau et al., 2018; Müller and Stein, 2014), when ocean circulation advected more heat towards the north (McManus et al., 2004; Rasmussen et al., 2012; Risebrobakken et al., 2011). This warm Atlantic water may play a role in the formation of first-year sea ice on the Yermak Plateau. Today, warm water sourced from the West Spitsbergen Current is diving underneath the sea ice. A source of warm water under the sea ice helps to break up the often-dense sea ice cover on the Yermak Plateau. This process creates leads in the sea ice, environments where first-year sea ice can form once it is cold enough again.

5. Conclusions

In this study we aimed to shed light on the presence of first-year sea ice in the Yermak Plateau over the last ca. 50 cal kyr BP. We used the approach of Pgla-DNA, a genetic proxy targeting the sea ice dwelling dinoflagellate *Polarella glacialis*, which reflects first- year sea ice in the Arctic. We find that Pgla-DNA is present in low abundance during MIS 3 and was present back to ca. 50,000 years ago on the Yermak Plateau, representing one of the oldest records so far and confirming previous reports on the stratigraphic range of *P. glacialis*. Our results support that Pgla-DNA is not commonly found in a multi-year sea ice environment, but more abundantly present in a seasonal sea ice environment. Until ca. 17 cal kyr BP, no first-year sea ice occurred in the dominantly multi-year sea ice environment on the Yermak Plateau. The limited amount of both biomarkers and Pgla-DNA in the sediments, shows that after 17 cal kyr BP the Yermak Plateau then experienced cold conditions with minimal sea ice melt. Since 17 cal kyr BP, a seasonal sea ice environment was established, but first-year sea ice did not occur until 15.4 cal kyr BP. First-year sea ice and the seasonal sea ice cover was very variable throughout the Bølling-Allerød, with the environment being either seasonally sea ice covered or even sea ice free. Nevertheless, except for a short period of a permanent sea ice cover during the Younger Dryas, first-year sea ice became a common feature on the Yermak Plateau from ca. 13.8 cal kyr BP onwards.

Both Pgla-DNA and the sea ice biomarker IP_{25} increased from the early Holocene (warm) to the late Holocene (cool), which may be related to the regional cooling trend and affected by changes with the inflow of warm "Atlantic" water, leading to the formation of a first-year sea ice rather than multi-year sea ice environment.

In the future Arctic, it is expected that first-year sea ice will replace multi-year sea ice, and this will have consequences for the ecosystem. Our work supports the usefulness of the newly proposed Pgla-DNA proxy (Hardardóttir et al., 2024) to reconstruct first-year sea ice. With this proxy, we have now documented a transition from multi-year ice (deglaciation) without first-year sea ice, to an environment with seasonal sea ice and first-year ice (Holocene). Further investigations on how the ecosystem has changed from the multi-year sea ice to first-year sea ice setting will provide information how a future Arctic Ocean might function.

Data statement

The magnetic susceptibility, radiocarbon and Pgla-DNA data from KH21-234-34GC have been submitted to PANGAEA and are also available from Mendeley Data at doi: 10.17632/fw7sk26r3p.1.

Data from PS2837-5 is available from www.pangaea.de, specifically the magnetic susceptibility data of Niessen (2000) at doi:10.1594/PANGAEA.57656; the radiocarbon ages from Nørgaard-Pedersen et al. (2003) at doi:10.1594/PANGAEA.104834; and the IP_{25} concentration from Müller et al. (2009) at doi:10.1594/PANGAEA.728973 and the brassicasterol concentration from Birgel and Hass (2004) at doi:10.1594/PANGAEA.193704.

CRediT authorship contribution statement

Kyle Michael James Mayers: Writing – review & editing, Writing – original draft, Methodology, Investigation, Formal analysis, Data curation, Conceptualization. **Nele Manon Vollmar:** Writing – review & editing. **Tristan Cordier:** Writing – review & editing, Methodology. **Agnes Katharina Maria Weiner:** Writing – review & editing, Methodology. **Juliane Müller:** Writing – review & editing, Validation, Methodology, Formal analysis, Data curation. **Aud Larsen:** Writing – review & editing. **Stijn De Schepper:** Writing – review & editing, Writing – original draft, Visualization, Resources, Project administration, Methodology, Investigation, Funding acquisition, Formal analysis, Data curation, Conceptualization.

Declaration of competing interest

This study was funded by the European Union, ERC Consolidator Grant AGENSI (818449) and ERC Synergy Grant i2B (101118519). Views and opinions expressed are however those of the author(s) only and do not necessarily reflect those of the European Union or the European Research Council Executive Agency. Neither the European Union nor the granting authority can be held responsible for them. There are no additional relationships to disclose, no patents to disclose, and no additional activities to disclose.

Acknowledgements

We would like to thank the crew of RV Kronprins Haakon during cruise KH21-234. We thank Katja Häkli, Sigrid Mugu, Dag Inge Blindheim (NORCE) and Stig Monsen (UiB) for technical support and Margit Simon for the help with obtaining the 14C ages from the ETH Zürich radiocarbon lab. This study was funded by the European Union, ERC Consolidator Grant AGENSI (818449) and ERC Synergy Grant i2B (101118519). Views and opinions expressed are however those of the author(s) only and do not necessarily reflect those of the European Union or the European Research Council Executive Agency. Neither the European Union nor the granting authority can be held responsible for them. We would also like to thank two anonymous reviewers whose comments improved the manuscript.

Supplementary materials

Supplementary material associated with this article can be found, in the online version, at doi:10.1016/j.epsl.2025.119809.

Data availability

The magnetic susceptibility, radiocarbon and Pgla-DNA data from KH21-234-34GC have been submitted to PANGAEA and are also available from Mendeley Data at doi: 10.17632/fw7sk26r3p.1.

References

Birgel, D., Hass, H.C., 2004. Oceanic and atmospheric variations during the last deglaciation in the Fram Strait (Arctic Ocean): a coupled high-resolution organic-geochemical and sedimentological study. Quat. Sci. Rev. 23, 29–47. https://doi.org/10.1016/j.quascirev.2003.10.001.

Boere, A.C., Abbas, B., Rijpstra, W.I.C., Versteegh, G.J.M., Volkman, J.K., Sinninghe Damsté, J.S., Coolen, M.J.L., 2009. Late-Holocene succession of dinoflagellates in an Antarctic fjord using a multi-proxy approach: paleoenvironmental genomics, lipid biomarkers and palynomorphs. Geobiology 7, 265–281. https://doi.org/10.1111/j.1472-4669.2009.00202.x.

Brendryen, J., Haflidason, H., Yokoyama, Y., Haaga, K.A., Hannisdal, B., 2020. Eurasian Ice Sheet collapse was a major source of meltwater pulse 1A 14,600 years ago. Nat. Geosci. 13, 363–368. https://doi.org/10.1038/s41561-020-0567-4.

Chauhan, T., Rasmussen, T.L., Noormets, R., Jakobsson, M., Hogan, K.A., 2014. Glacial history and paleoceanography of the southern Yermak Plateau since 132 ka BP. Quat. Sci. Rev. 92, 155–169. https://doi.org/10.1016/j.quascirev.2013.10.023.

Comiso, J.C., Parkinson, C.L., Gersten, R., Stock, L., 2008. Accelerated decline in the Arctic sea ice cover. Geophys. Res. Lett. 35, 2007GL031972. https://doi.org/10.1029/2007GL031972.

Dell'Anno, A., Corinaldesi, C., 2004. Degradation and turnover of extracellular DNA in marine sediments: ecological and methodological considerations. Appl. Environ. Microbiol. 70 (7), 4384–4386. https://doi.org/10.1128/AEM.70.7.4384-4386.2004.

De Schepper, S., Ray, J.L., Skaar, K.S., Sadatzki, H., Ijaz, U.Z., Stein, R., Larsen, A., 2019. The potential of sedimentary ancient DNA for reconstructing past sea ice evolution. ISMe J. 13, 2566–2577. https://doi.org/10.1038/s41396-019-0457-1.

de Vernal, A., Gersonde, R., Goosse, H., Seidenkrantz, M.-S., Wolff, E.W., 2013. Sea ice in the paleoclimate system: the challenge of reconstructing sea ice from proxies – an introduction. Quat. Sci. Rev. 79, 1–8. https://doi.org/10.1016/j.quascirev.2013.08.009.

de Vernal, A., Radi, T., Zaragosi, S., Van Nieuwenhove, N., Rochon, A., Allan, E., De Schepper, S., Eynaud, F., Head, M.J., Limoges, A., Londeix, L., Marret, F., Matthiessen, J., Penaud, A., Pospelova, V., Price, A., Richerol, T., 2020. Distribution of common modern dinoflagellate cyst taxa in surface sediments of the Northern Hemisphere in relation to environmental parameters: the new n=1968 database.

Mar. Micropaleontol. 159, 101796. https://doi.org/10.1016/j.marmicro.2019.101796.
Deb, J.C., Bailey, S.A., 2023. Arctic marine ecosystems face increasing climate stress. Env. Rev. 31, 403–451. https://doi.org/10.1139/er-2022-0101.
El bani Altuna, N., Ezat, M.M., Smik, L., Muschitiello, F., Belt, S.T., Knies, J., Rasmussen, T.L., 2024. Sea ice-ocean coupling during Heinrich Stadials in the Atlantic–Arctic gateway. Sci. Rep. 14, 1065. https://doi.org/10.1038/s41598-024-51532-7.
Falardeau, J., De Vernal, A., Spielhagen, R.F., 2018. Paleoceanography of northeastern Fram Strait since the last glacial maximum: palynological evidence of large amplitude changes. Quat. Sci. Rev. 195, 133–152. https://doi.org/10.1016/j.quascirev.2018.06.030.
Farnsworth, W.R., Allaart, L., Ingólfsson, Ó., Alexanderson, H., Forwick, M., Noormets, R., Retelle, M., Schomacker, A., 2020. Holocene glacial history of Svalbard: status, perspectives and challenges. Earth-Sci. Rev. 208, 103249. https://doi.org/10.1016/j.earscirev.2020.103249.
Fetterer, F., Knowles, K., Meier, W., Savoie, M., Windnagel, A.K., 2017. Sea Ice Index, Version 3 [Sea_Ice_Index_Monthly_Data_ with_Statistics_G02135_v3.0]. NSIDC: National Snow and Ice Data Center, Boulder, Colorado USA.
Figueroa, R.L., Dapena, C., Bravo, I., Cuadrado, A., 2015. The hidden sexuality of Alexandrium Minutum: an example of overlooked sex in dinoflagellates. PLoS. One 10 (11), e0142667. https://doi.org/10.1371/journal.pone.0142667.
Flores, H., Veyssière, G., Castellani, G., Wilkinson, J., Hoppmann, M., Karcher, M., Valcic, L., Cornils, A., Geoffroy, M., Nicolaus, M., Niehoff, B., Priou, P., Schmidt, K., Stroeve, J., 2023. Sea-ice decline could keep zooplankton deeper for longer. Nat. Clim. Chang 1–9. https://doi.org/10.1038/s41558-023-01779-1.
Godhe, A., Asplund, M.E., Härnström, K., Saravanan, V., Tyagi, A., Karunasagar, I., 2008. Quantification of diatom and dinoflagellate biomasses in coastal marine seawater samples by real-time PCR. Appl. Environ. Microbiol. 74 (23), 7174–7182. https://doi.org/10.1128/AEM.01298-08.
Gradinger, R, Friedrich, C, Spindler, M, 1999. Abundance, biomass and composition of the sea ice biota of the Greenland Sea pack ice. Deep Sea Res II 46, 1457–1472.
Hald, M. and Aspeli, R., Rapid shifts of the norther Norwegian Sea during the last deglaciation and the holocene, Boreas, 1997, vol. 26, pp. 15–28.
Harðardóttir, S., Haile, J.S., Ray, J.L., Limoges, A., Van Nieuwenhove, N., Lalande, C., Grondin, P.-L., Jackson, R., Skaar, K.S., Heikkilä, M., Berge, J., Lundholm, N., Massé, G., Rysgaard, S., Seidenkrantz, M.-S., De Schepper, S., Lorenzen, E.D., Lovejoy, C., Ribeiro, S., 2024. Millennial-scale variations in Arctic sea ice are recorded in sedimentary ancient DNA of the microalga Polarella glacialis. Commun. Earth Env. 5, 25. https://doi.org/10.1038/s43247-023-01179-5.
Haslett, J., Parnell, A., 2008. A simple monotone process with application to radiocarbon-dated depth chronologies. J. R. Stat. Soc.: C 57, 399–418. https://doi.org/10.1111/j.1467-9876.2008.00623.x.
Heaton, T.J., Köhler, P., Butzin, M., Bard, E., Reimer, R.W., Austin, W.E.N., Ramsey, C.B., Grootes, P.M., Hughen, K.A., Kromer, B., Reimer, P.J., Adkins, J., Burke, A., Cook, M. S., Olsen, J., Skinner, L.C., 2020. Marine20—The Marine radiocarbon age calibration curve (0–55,000 cal BP). Radiocarbon 62, 779–820. https://doi.org/10.1017/RDC.2020.68.
Heikkilä, M., et al., 2014. Surface sediment dinoflagellate cysts from the Hudson Bay system and their relation to freshwater and nutrient cycling. Mar. Micropaleontol 106, 79–109.
Hindson, B.J., Ness, K.D., Masquelier, D.A., Belgrader, P., Heredia, N.J., Makarewicz, A. J., Bright, I.J., Lucero, M.Y., Hiddessen, A.L., Legler, T.C., Kitano, T.K., Hodel, M.R., Petersen, J.F., Wyatt, P.W., Steenblock, E.R., Shah, P.H., Bousse, L.J., Troup, C.B., Mellen, J.C., Colston, B.W., 2011. High-throughput droplet digital PCR system for absolute quantitation of DNA copy number. Anal. Chem. 83 (22), 8604–8610. https://doi.org/10.1021/ac202028g.
Hop, H., Vihtakari, M., Bluhm, B.A., Assmy, P., Poulin, M., Gradinger, R., Peeken, I., von Quillfeldt, C., Olsen, L.M., Zhitina, L., Melnikov, I.A., 2020. Changes in sea-ice protist diversity with declining sea ice in the Arctic Ocean from the 1980s to 2010s. Front. Mar. Sci. 7. https://doi.org/10.3389/fmars.2020.00243.
Jahn, A., Holland, M.M., Kay, J.E., 2024. Projections of an ice-free Arctic Ocean. Nat. Rev. Earth Env. 5, 164–176. https://doi.org/10.1038/s43017-023-00515-9.
Jokat, W., 1999. The expedition ARKTIS-XV/2 of "Polarstern" in 1999 (No. 368). Berichte zur Polar- und Meeresforschung. Alfred Wegener Institute for Polar and Marine Research, Bremerhaven.
Kauko, H.M., Olsen, L.M., Duarte, P., Peeken, I., Granskog, M.A., Johnsen, G., Fernández-Méndez, M., Pavlov, A.K., Mundy, C.J., Assmy, P., 2018. Algal colonization of young Arctic Sea ice in spring. Front. Mar. Sci. 5, 199. https://doi.org/10.3389/fmars.2018.00199.
Kokkoris, V., Vukicevich, E., Richards, A., Thomsen, C., Hart, M.M., 2021. Challenges using droplet digital PCR for environmental samples. Appl. Microbiol. 1 (1), 74–88. https://doi.org/10.3390/applmicrobiol1010007.
Krabberød, A.K., Stokke, E., Thoen, E., Skrede, I., Kauserud, H., 2025. The Ribosomal operon database: A full-length <scp>rDNA</scp>operon database derived from genome assemblies. Mol. Ecol. Resour. 25. https://doi.org/10.1111/1755-0998.14031.
Kremer, A., Stein, R., Fahl, K., Bauch, H., Mackensen, A., Niessen, F., 2018. A 190-ka biomarker record revealing interactions between sea ice, Atlantic Water inflow and ice sheet activity in eastern Fram Strait. Arktos 4, 1–17. https://doi.org/10.1007/s41063-018-0052-0.
Kwok, R., 2018. Arctic sea ice thickness, volume, and multiyear ice coverage: losses and coupled variability (1958–2018). Env., Res. Lett. 13, 105005. https://doi.org/10.1088/1748-9326/aae3ec.
Lavrinienko, A., Jernfors, T., Koskimäki, J.J., Pirttilä, A.M., Watts, P.C., 2021. Does intraspecific variation in rDNA copy number affect analysis of microbial communities? Trends. Microbiol. 29, 19–27. https://doi.org/10.1016/j.tim.2020.05.019.
Limoges, A., Ribeiro, S., Weckström, K., Heikkilä, M., Zamelczyk, K., Andersen, T.J., Tallberg, P., Massé, G., Rysgaard, S., Nørgaard-Pedersen, N., Seidenkrantz, M., 2018. Linking the modern distribution of biogenic proxies in high Arctic Greenland Shelf sediments to sea ice, primary production, and Arctic-Atlantic inflow. JGR Biogeosciences 123, 760–786. https://doi.org/10.1002/2017JG003840.
Limoges, A., Van Nieuwenhove, N., Head, M.J., Mertens, K.N., Pospelova, V., Rochon, A., 2020. A review of rare and less well known extant marine organic-walled dinoflagellate cyst taxa of the orders Gonyaulacales and Suessiales from the Northern Hemisphere. Mar. Micropaleontol. 159, 101801. https://doi.org/10.1016/j.marmicro.2019.101801.
Lucchi, R.G., Sagnotti, L., Camerlenghi, A., Macrì, P., Rebesco, M., Pedrosa, M.T., Giorgetti, G., 2015. Marine sedimentary record of Meltwater Pulse 1a along the NW. Barents Sea Cont. Margin, Arktos 1, 7. https://doi.org/10.1007/s41063-015-0008-6.
Mäkelä, M., Luostarinen, T., Ribeiro, S., Weckström, K., Sejr, M., Winding, M., Heikkilä, M., 2025. Diatom and dinoflagellate cyst fluxes over four annual cycles in a high arctic fjord, Northeast Greenland. Glob. Biogeochem. Cycles 39, 7. https://doi.org/10.1029/2024GB008478.
Marret, F., Bradley, L., De Vernal, A., Hardy, W., Kim, S.-Y., Mudie, P., Penaud, A., Pospelova, V., Price, A.M., Radi, T., Rochon, A., 2020. From bi-polar to regional distribution of modern dinoflagellate cysts, an overview of their biogeography. Mar. Micropaleontol. 159, 101753. https://doi.org/10.1016/j.marmicro.2019.101753.
McManus, J.F., Francois, R., Gherardi, J.-M., Keigwin, L.D., Brown-Leger, S., 2004. Collapse and rapid resumption of Atlantic meridional circulation linked to deglacial climate changes. Nature 428, 834–837. https://doi.org/10.1038/nature02494.
Montresor, M., Procaccini, G., Stoecker, D.K., 1999. Polarella glacialis, Gen. Nov., sp. Nov (Dinophyceae): Suessiaceae are still alive. J. Phycol. 35, 186–197.
Montresor, M., Lovejoy, C., Orsini, L., Procaccini, G., Roy, S., 2003. Bipolar distribution of the cyst-forming dinoflagellate Polarella glacialis. Polar Biol 26, 186–194.
Müller, J., Massé, G., Stein, R., Belt, S.T., 2009. Variability of sea-ice conditions in the Fram Strait over the past 30,000 years. Nat. Geosci. 2, 772–776. https://doi.org/10.1038/ngeo665.
Müller, J., Stein, R., 2014. High-resolution record of late glacial and deglacial sea ice changes in Fram Strait corroborates ice–ocean interactions during abrupt climate shifts. Earth Planet. Sci. Lett. 403, 446–455. https://doi.org/10.1016/j.epsl.2014.07.016.
Müller, J., Wagner, A., Fahl, K., Stein, R., Prange, M., Lohmann, G., 2011. Towards quantitative sea ice reconstructions in the northern North Atlantic: A combined biomarker and numerical modelling approach. Earth Planet. Sci. Lett. 306, 137–148. https://doi.org/10.1016/j.epsl.2011.04.011.
Niessen, F., 2000. Physical properties of sediment core PS2837-5. doi:10.1594/PANGAEA.57656.
Nørgaard-Pedersen, N., Spielhagen, R.F., Erlenkeuser, H., Grootes, P.M., Heinemeier, J., Knies, J., 2003. Arctic Ocean during the Last Glacial Maximum: Atlantic and polar domains of surface water mass distribution and ice cover. Paleoceanography 18, 2002PA000781. https://doi.org/10.1029/2002PA000781.
Pieńkowski, A.J., Szczuciński, W., Breszka, A., Chyleński, M., Juras, A., Romel, P., Rozwalak, P., Trzebny, A., Dabert, M., Belt, S.T., Jagodziński, R., Smik, L., Włodarski, W., 2024. Sedimentary ancient DNA and HBI biomarkers as sea-ice indicators: A complementary approach in Antarctic fjord environments. Limnol Ocean. Lett. lol2, 10395. https://doi.org/10.1002/lol2.10395.
Rasmussen, T.L., Forwick, M., Mackensen, A., 2012. Reconstruction of inflow of Atlantic Water to Isfjorden, Svalbard during the Holocene: correlation to climate and seasonality. Mar. Micropaleontol. 94–95, 80–90. https://doi.org/10.1016/j.marmicro.2012.06.008.
Risebrobakken, B., Dokken, T., Smedsrud, L.H., Andersson, C., Jansen, E., Moros, M., Ivanova, E.V., 2011. Early Holocene temperature variability in the Nordic Seas: the role of oceanic heat advection versus changes in orbital forcing. Paleoceanography 26, 2011PA002117. https://doi.org/10.1029/2011PA002117.
Stein, Ruediger, Fahl, Kirsten, Grobe, Hannes, 2003. Documentation of sediment core PS2837-5. Alfred Wegener Institute - Polarstern core repository. https://doi.org/10.1594/PANGAEA.115536. PANGAEA</Dataset>.
Stoecker, D., Gustafson, D.E., Black, M.M.D., Baier, C.T., 1998. Population dynamics of microalgae in the upper land-fast sea ice at a snow free location. J. Phycol. 34, 60–69.
Stroeve, J., Meier, W.N., 2018. *Sea Ice Trends and Climatologies from SMMR and SSM/I-SSMIS, Version 3*. [Indicate subset used]. NASA National Snow and Ice Data Center Distributed Active Archive Center, Boulder, Colorado USA. https://doi.org/10.5067/IJ0T7HFHB9Y6 [Date Accessed].
Veres, D., Bazin, L., Landais, A., Toyé Mahamadou Kele, H., Lemieux-Dudon, B., Parrenin, F., Martinerie, P., Blayo, E., Blunier, T., Capron, E., Chappellaz, J., Rasmussen, S.O., Severi, M., Svensson, A., Vinther, B., Wolff, E.W., 2013. The Antarctic ice core chronology (AICC2012): an optimized multi-parameter and multi-site dating approach for the last 120 thousand years. Clim. Past 9, 1733–1748. https://doi.org/10.5194/cp-9-1733-2013.
Vogelsang, E., Sarnthein, M., Pflaumann, U., Vogelsang, E., et al., 2003. Age control of sediment core PS2837-5. In supplement to: Vogelsang, E et al. (2001): d18O Stratigraphy, chronology, and sea surface temperatures ofAtlantic sediment records (GLAMAP-2000 Kiel). Berichte-Reports, 13. Institut für Geowissenschaften, Universität Kiel, p. 13. https://doi.org/10.1594/PANGAEA.104834. +244//doi.org/10.2312/reports-ifg.2001.13.
Walsh, J.E., Fetterer, F., Scott Stewart, J., Chapman, W.L., 2017. A database for depicting Arctic sea ice variations back to 1850. Geogr. Rev. 107, 89–107. https://doi.org/10.1111/j.1931-0846.2016.12195.x.

Werner, I., Ikävalko, J., Schünemann, H., 2007. Sea-ice algae in Arctic pack ice during late winter. Polar Biol 30, 1493–1504.

Xiao, X., Stein, R., Fahl, K., 2015. MIS 3 to MIS 1 temporal and LGM spatial variability in Arctic Ocean sea ice cover: reconstruction from biomarkers. Paleoceanography 30, 969–983. https://doi.org/10.1002/2015PA002814.

Zhu, F., Massana, R., Not, F., Marie, D., Vaulot, D., 2005. Mapping of picoeucaryotes in marine ecosystems with quantitative PCR of the 18S rRNA gene. FEMS Microbiol. Ecol. 52, 79–92. https://doi.org/10.1016/j.femsec.2004.10.006.

Zonneveld, K.A.F., Marret, F., Versteegh, G.J.M., Bogus, K., Bonnet, S., Bouimetarhan, I., Crouch, E., De Vernal, A., Elshanawany, R., Edwards, L., Esper, O., Forke, S., Grøsfjeld, K., Henry, M., Holzwarth, U., Kielt, J.-F., Kim, S.-Y., Ladouceur, S., Ledu, D., Chen, L., Limoges, A., Londeix, L., Lu, S.-H., Mahmoud, M.S., Marino, G., Matsouka, K., Matthiessen, J., Mildenhal, D.C., Mudie, P., Neil, H.L., Pospelova, V., Qi, Y., Radi, T., Richerol, T., Rochon, A., Sangiorgi, F., Solignac, S., Turon, J.-L., Verleye, T., Wang, Y., Wang, Z., Young, M., 2013. Atlas of modern dinoflagellate cyst distribution based on 2405 data points. Rev. Palaeobot. Palynol. 191, 1–197. https://doi.org/10.1016/j.revpalbo.2012.08.003.